Impact of Morphological Orientation in Determining Mechanical Properties in Triblock Copolymer Systems

Christian C. Honeker and Edwin L. Thomas*

Department of Materials Science & Engineering, Massachusetts Institute of Technology, Cambridge, Massachusetts 02139

Received February 23, 1996. Revised Manuscript Received June 12, 1996[⊗]

In contrast to other types of segmented multiblock thermoplastic elastomers, simple ABA block copolymers represent a class of well-defined nanostructured materials. Due to the inherent block lengths built in during the polymerization, the microdomain structure of block copolymers exhibits a size scale of typically 10−100 nm. The ability to control the individual chemistry of each block as well as the size and the shape of the domains in a block copolymer affords enormous advantages to tailor physical properties. By globally orienting the microdomains, a well-defined initial morphological state aids greatly in the interpretation and modeling of mechanical deformation and allows for exploitation of the inherent anisotropy of the cylindrical and lamellar structures. Several types of orientation techniques are reviewed. Experiments investigating structure−mechanical properties in styrene−diene triblock copolymers with spherical, cylindrical, and lamellar morphologies are discussed, with emphasis on the clarifying role of global morphological orientation in data interpretation. Composite theory which treats each microphase as a continuum describes small strain behavior of cylinders and lamellae quite well. Molecular variables such as the number of effective bridge vs loop conformations in the rubber midblock become more important at large strains. With controlled chemistry and morphology as well as with improved dynamic probes, further understanding between the interplay of molecular and morphological structure in influencing the deformation process is expected.

I. Introduction

In keeping with the nanostructural theme of this special issue, this review will examine the role of morphological orientation in the investigation of the mechanical properties of multiphase polymer systems. Thermoplastic elastomers (TPEs) represent a class of multiphase polymers which have a typical domain structure on the 10 nm length scale and a typical grain structure on a 1000 nm length scale. There are four main TPE materials of commercial importance each consisting of a hard block (crystalline or glassy) coupled to a rubbery soft block: polystyrene/elastomer, polyurethane/elastomer, polyester/elastomer, polyamide/elastomer. The former is a simple triblock, while the latter three are made up of segmented multiblocks of the indicated constituents. In addition, TPEs can be made by the fine-scale blending of a hard thermoplastic with an elastomer.[1,2] The common feature of a TPE is the presence of a soft domain, which gives rise to the elastomeric nature of the material, in intimate contact with a hard domain, which increases the modulus and enhances the mechanical integrity of the composite material. A key attribute of most TPEs is the ability to tailor toughness and large strain elasticity by varying the ratio of hard/soft fractions. Upon the addition of heat and/or solvent, a TPE system becomes reversibly homogeneous and processible. The growing commercial importance of TPEs is reflected in the worldwide non-tire rubber market share which stands at 11% with 420 000 tons. This share is expected to double and production to increase to 550 000 tons in the next 5 years.[3]

I.1. Structure of a Model TPE.

In this article we concern ourselves with perhaps the most ideal class of TPEs, namely, that of polystyrene/polydiene/polystyrene ABA triblock copolymers.

In block copolymers there are basically three levels of structure:

(i) The local chemical microstructure of the blocks.

(ii) The size and shape of the microdomains.

(iii) The superstructure of the grains.

Figure 1 illustrates this hierarchical structure for a triblock comprised of a majority of polybutadiene (PB) and a minority of polystyrene (PS). The monomeric repeat units are shown with a scale bar of 0.5 nm. Typically hundreds of such units make up each respective block. Both blocks are noncrystalline so that it is only the incompatibility of the two monomers which drives the self-assembly into A-rich and B-rich microdomains. The size and shape of the microdomains are dictated primarily by the relative volume fractions of the two blocks; in the schematic shown, the minority glassy PS block forms cylindrical microdomains embedded in the majority rubbery PB matrix. These cylindrical microdomains which are comprised of a PS interior and are surrounded by a polybutadiene corona, in turn, assemble themselves onto a 2-D hexagonal lattice. Two types of conformations are shown for the rubbery midblock: loops and effective bridges (which include catenated loops) which are key for stress transfer between the glassy domains. If, in preparing a bulk sample, the self-assembly process occurs quiescently, (that is, without the application of any sort of hydrodynamic flow or electromagnetic fields) then small regions of parallel cylinders randomly nucleate and grow until

[⊗] Abstract published in *Advance ACS Abstracts,* August 1, 1996.

S0897-4756(96)00146-9 CCC: $12.00

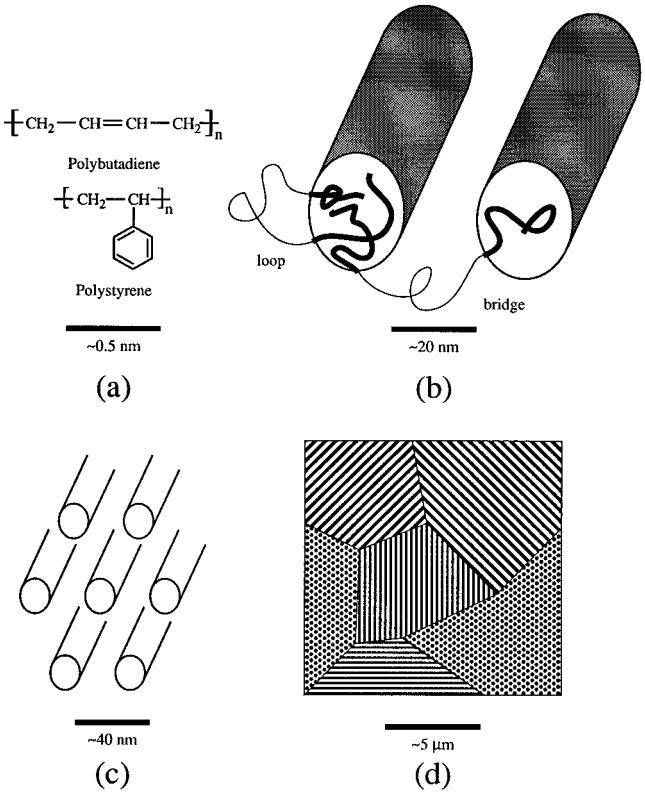

Figure 1. Structure of an ABA triblock copolymer viewed on several length scales. (a, b) Synthetic variables determine structure at the smallest length scales. (c, d) The microdomain geometry (in this case, hexagonally packed cylinders), grain size, and orientation are some examples of important morphological variables.

impingement. These impinged regions form a grain structure much like a polycrystalline material. Grains typically contain hundreds of cylinders. Just as in other crystalline materials, minimization of high-energy grain boundaries drives grain growth when the system is annealed above the glass transition temperature of the higher T_g block.

Grain sizes of block copolymers are usually in the 1−10 μm range[4] so that a macroscopic sample of copolymer (>1 mm) will generally exhibit isotropic properties. If an applied bias field is present during the self-assembly process, then instead of random nucleation of the microdomains a single-crystal-like orientation can develop. Another way to develop a highly aligned structure is to texture an initial random polygrain structure by application of a bias field to the already microphase-separated state. Section II describes a number of processes which achieve aligned structures to varying degrees.

I.2. Structure−Property Relationships. An ideal investigation of the structure−mechanical property relation in block copolymer involves several aspects:

(i) Control of synthetic and morphological variables.

(ii) Application of molecular and morphological characterization tools to assess initial morphology and to follow the evolution of the morphology as a function of stress, strain, strain rate, temperature, and other mechanical variables.

Since the main features of the styrene−diene composition−morphology diagram in the strong segregation limit (with χN large, where χ represents the incompatibility between dissimilar monomers and N the molecular weight of the polymer) were first outlined in 1970,[5] it is possible to predict what the equilibrium microdomain structure should be *based on composition alone*. This has several advantages in block copolymer deformation studies. Polymer chemists are thus able to reproducibility synthesize a molecule with the desired microdomain structure. Second, models useful with interpretation of deformation results can be constructed based on the appropriate microdomain geometry. Unfortunately, many deformation studies,[6−12] even recent ones,[13,14] have not paid sufficient attention to whether or not a sample has achieved the equilibrium microdomain structure or to whether the sample is globally aligned. Solvent casting, especially for highly volatile, preferential solvents, is known to induce nonequilibrium metastable microdomain structures, and many early studies[6−8,10] are of limited value since they measure the mechanical properties resulting from metastable samples. However, with the appropriate annealing regimen, it is possible in most cases, to drive the system to microdomain equilibrium even in samples cast from preferential solvents. However, to get a global equilibrium morphology, i.e., a sample consisting of a single large grain composed of well-ordered microdomains, processing is needed. In any case, a check of the initial morphology should be performed so that a proper setting for further interpretation is provided, even in studies of mechanical properties not emphasizing the role of morphology.

I.3. Importance of Large-Scale Morphology. Often after a new polymer is synthesized, preliminary experiments are performed to determine the material's properties. In attempts to understand the link between the molecular structure of a material (e.g., the chemical nature of the constituents in the new polymer) and its physical characteristics, measurements generally include some type of deformation experiment to extract mechanical information, since it will often be the mechanical properties of the new material that determine its commercial usage. Presently, polymer chemists are still far from being able to design polymers with the appropriate mechanical properties, although the field of polymer science and engineering has come a long way toward this goal. Mechanical properties, such as modulus, toughness, and strength, however, depend on much more than the chemistry, molecular microstructure, and local conformation of the polymer chain. Structures on larger length scales such as grains, grain boundaries, and isolated line defects can mask or even dominate the response of the material to a mechanical stimulus. These larger scale structural aspects, and in turn the macroscopic properties, are significantly influenced by the processing history of the sample even after the molecular characteristics have been prescribed. To better understand the impact on macroscopic mechanical properties of introducing or replacing a particular side group or incorporating a novel monomeric species, it is necessary to more directly link the molecular response to the macroscopic stimulus. This can be done by controlling the morphology (i.e., through orientation) so that the potential obscuring effects of the above-mentioned supermolecular defect structures are reduced. The techniques used to manipulate morphology rely on the ability to couple an externally applied field to some molecular and/or supermolecular feature in the

polymer. A brief discussion of these orientation techniques follows.

II. Orientation Methods

There are many ways to couple an external field to a polymer system for the purpose of inducing microdomain orientation. Most mechanical means rely on a hydrodynamic flow field to influence the domain structure, either through stress transfer to the stiffer microdomain component or through a perturbation of the overall chain conformation prior to microdomain formation. Electrical and magnetic fields can provide a molecular stimulus through the dielectric and diamagnetic anisotropy of the monomeric units as well as a morphological stimulus through a composition-dependent variation of the dielectric constant.[15,16] In contrast to the strong effect of flow fields, the driving force for electric or magnetic field-induced orientation is weak.

A particular orientation method in most studies of block copolymers is chosen for one of two reasons: to study the orientation method itself or as a convenient means to prepare oriented samples for further study. The fluid dynamics of the various hydrodynamic flow field techniques can be quite complex and have been reviewed.[17] Here, emphasis will be placed on the various methods as a tool for preparing samples for subsequent deformation study. One restriction in considering these techniques for orienting morphologies is that the resultant samples should have a uniform orientation throughout a volume large enough for tensile testing.

II.1. Extrusion. Extrusion is a common commercial processing method for thermoplastic elastomers;[18,19] several attempts at relating the orientation due to the processing to the structure have been made.[20−22] The most successful investigation was carried out by Keller and co-workers, who were the first to apply extrusion to orient a block copolymer. They demonstrated dramatic success in inducing global orientation in extruded plugs of a poly(styrene-butadiene-styrene) (SBS).[23,123] Molten (but still microphase-separated) material was squeezed through an orifice into a heated glass capillary before being cooled to room temperature. Flow through the glass capillary was found to impart additional shear, enhancing the quality of orientation. Due to the variation in shear profile, however, the degree of orientation varied from the surface of the plug (where shear was highest) to the core (where shear was lowest). Nevertheless, full advantage of the macroscopic nature of the orientation was made in experiments probing mechanical properties, birefringence, and swelling behavior. Details of some of these pioneering deformation studies will be discussed in section IV.2.

II.2. Reciprocating Shear. A significant advancement in the techniques used to orient block copolymers was made by Skoulios and Hadziioannou with the introduction of a reciprocating shear apparatus.[24−27] The equipment consisted of two parallel plates with an adjustable gap. The block copolymer was sheared by the oscillatory motion of the bottom plate with respect to a stationary top plate. Both blocks were heated with shearing conducted under vacuum for several hours. The reciprocating shear technique has been recently revived[28−30] and is becoming a common technique for orientation.[31,32] One advantage to this technique is the simplicity of the flow field: simple shear. An example of this advantage is in the development of theory[33,34] that is able to predict the experimentally observed "flipping" transition of lamellae diblocks,[35] whereby the lamellar normals rotate from the shear gradient (parallel configuration) to the vorticity (perpendicular configuration) direction as the ODT is approached or shear rate increased.

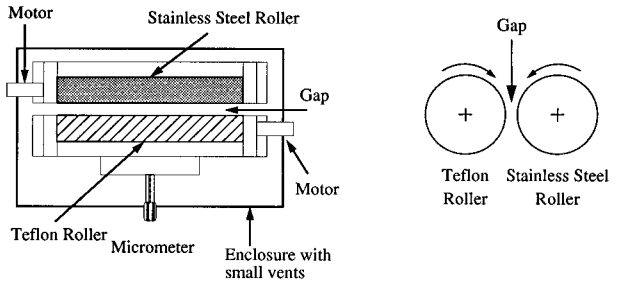

Figure 2. Left: schematic plan view of the Roll-Caster.[40] Two parallel rollers counterrotate at a fixed separation controlled by a micrometer. Right: cross-sectional view.

II.3. Press Molding. A common method used to orient block copolymers, but whose orientation mechanism is much less understood is press molding. Typically, the copolymer is heated and compressed to a desired thickness. The resulting biaxial flow field produces a film within which the morphology is radially oriented. Press molding has been typically applied to block copolymers with cylindrical morphology;[12,36−38] apparently, there is only one press-molding study carried out on block copolymers with lamellar morphology.[13]

II.4. Roll-Casting. A new orientation technique called "roll-casting" has recently been developed in our lab.[39−41] Roll-casting involves the slow evaporation of solvent from a homogeneous solution with the simultaneous application of a periodic flow field to produce films with an oriented morphology. The most important difference between roll-casting and the aforementioned orientation techniques is that the flow field is applied to a solution as opposed to an unoriented, microphase-separated solid above the glass transition of the hard block. As it might be anticipated for a microphase-separated system, the initial grain size and degree of domain alignment influences the final degree of global order in an orienting process.[42] By beginning with a homogeneous material and allowing the morphology to develop (i.e., inducing microphase separation) in the presence of the flow field, the final morphology can have superior orientation with fewer defects. To access the homogeneous state, a solvent is necessary for high molecular weight polymers since heating the material will lead to thermal decomposition before reaching the disordering temperature.

The essential features of the roll-caster are shown in Figure 2. Two (or three) parallel rollers, one of stainless steel and the other(s) of Teflon, counterrotate at a constant frequency ω. The rollers are separated from each other by a micrometer-controlled distance (gap) and are driven by independent motors at constant speed. Further experimental details can be found elsewhere.[40,41] Initially the solution uniformly coats both the Teflon and stainless steel rollers. As the solvent evaporates and the material becomes more viscous, a film preferentially forms on the stainless steel cylinder.

In comparison to the various orientation methods discussed above, the roll-casting method offers some distinct advantages:

(i) Problems associated with thermal degradation are minimized by roll-casting at room temperature (though heating is also possible).

(ii) Resulting films are large (e.g., 20 cm × 6 cm × 2 mm).

(iii) A large number of variables can be changed to influence the process.

(iv) The process occurs relatively quickly (e.g., within 45 min) and is unsophisticated.

Thus, inducing block copolymer orientation from an initially homogeneous solution represents an improvement over orienting an inhomogeneous solid heated above its glass transition in two respects: (1) orienting a developing structure results in fewer morphological defects than an established structure which has to be reoriented and (2) thermal degradation is minimized.

II.5. Other Orientation Methods. There are a number of other orientation methods available, but none as yet have been used to prepare samples for mechanical deformation studies.

1. Flow in a Rheometer. The application of an axisymmetric flow field to induce orientation in block copolymers using either parallel plate[43−50] or cone-and-plate rheometry[42] has been successful. Both cylinders[43−45] and lamellae[46−50] orient in the flow direction. Excellent control of shear strain, shear rate and temperature, and ease of measurement of shear stress during orientation are afforded. The flow field for the cone-and-plate geometry is well-characterized as simple shear, but the sample size is somewhat small for tensile testing purposes.

2. Couette Flow. This technique, pioneered by Terrisse,[51] has been used to orient block copolymer triblocks[52−54] and diblocks.[55,56] The device operates using the same principle as a couette viscometer with two concentric cylinders, one rotating with respect to the other. Recent studies using this technique have focused on the effects of shear on triblocks[52−54] and diblocks[55,56] near the order−disorder transition (ODT).

3. Electric Field. A fundamentally different method of orientation of block copolymers was first recognized by Le Meur[57] in observing light diffracting from highly solvent swollen lamellae subjected to electric fields (15 kV/cm). This technique operates on the principle that domains of differing dielectric constants respond differently to an electric field. The result is that a globally oriented structure represents a minimum in the electrostatic contribution to the free energy of the system. Amundson[15,16,58,59] also determined that weakly segregated lamellae orient parallel to the field. The driving force for morphological alignment in an electric field, however, is much smaller and the kinetics considerably slower (up to hundreds of minutes)[58] than that of a hydrodynamic flow.

4. Channel Die. This technique relies on a similar principle as press molding, but under conditions of plane strain. It involves the compressing of the "molten" material into a deep channel die. The material flows along one direction while being constrained in the other two. Semicrystalline block copolymers have been oriented using this technique,[60−62] but deformation studies have been carried out only on nylon 6,[63] polyethylene,[64,65] and poly(ethylene terephthalate) (PET).[66] Variable shear gradients due to the changing geometry during compression and the relatively short residence time under flow can lead to orientation gradients.

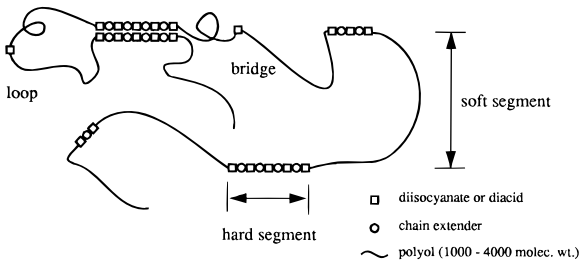

Figure 3. Schematic diagram of the chain architecture of a typical random multiblock copolymer molecule. The case shown is for a polyurethane/elastomer comprised of a hard segment based on diisocyanate or for a polyether ester comprised of a hard segment based on a diacid.

III. Segmented Multiblock Copolymers

There have been numerous developments in the synthesis of TPEs to optimize properties for particular applications.[1,18,19,67,68] Detailed studies on the interplay between molecular characteristics and morphological features in determining the macroscopic mechanical properties have been carried out, but for many reasons (most having to do with the degree of synthetic control; step vs anionic polymerization) morphological control of segmented multiblock copolymer systems is much more difficult than that of styrene/diene block copolymers. Consequently, the level of structure−property understanding is much greater in the latter case. Before focusing on simple ABA block copolymers, however, we remark briefly upon random block copolymers due to their commercial significance.

In segmented multiblock copolymers, such as polyurethanes and polyether esters, one of the units of the soft segment is usually an oligomer of 1000−4000 molecular weight. This oligomer is linked into a multiblock chain of alternating hard and soft sequences, each chain containing from 10 to 100 blocks (see Figure 3). Rather than by precisely controlled anionic polymerization, these materials are typically made by a rapid bulk step growth polymerization, which leads to a significant distribution in the compositions and molecular weights of copolymer molecules. As an example, consider polyurethane elastomers. There are two main procedures of synthesis. The first is the prepolymer method in which a prepolymerized soft segment (either a polyether or polyester) is reacted with a prepolymerized polyurethane. The second is the one shot method in which the soft segment (macrodiol) is mixed with a chain extender (diol) and a diisocyanate.[69−71] The first method gives a narrower distribution of hard segment lengths, because the prepolymer has a Flory distribution in molecular weight.[72] In the one-shot method, simultaneous reaction of the three species leads to a competition between the chain extender and soft segment for the diisocyanate. Even in the case where the soft segment is anionically polymerized (e.g., a polybutadiene soft segment), the hard segment is always polydisperse.[69]

In both polymerization methods, the final molecular (and thus morphological) makeup of a segmented multi-

block thermoplastic elastomer is extremely sensitive to the reaction conditions and processing. As the molecular weight increases, the hard segments and soft segments become incompatible, thereby phase separating, and the linking reactions occur at the phase boundary, which can upset the local stoichiometry. This may be problematic, for if the polymers are to achieve a high molecular weight, precise stoichiometry must be maintained. Temperature and molecular weight can influence the relative reactivity of the various components, which would broaden the molecular weight. Finally, both the glass transition and crystallization can hinder or stop the polymerization reaction if T_g and/or T_c of the hard domains reach the polymerization temperature. Solution polymerization can alleviate some of these difficulties, but the potential for polymer−solvent interactions is introduced, which would present a new set of polymerization variables and problems. Recently, however, an effort has been made to synthesize model polyurethanes with well-defined segment length distributions thus enabling a control of the morphology not unlike that found in anionically synthesized block copolymers.[73,74]

In addition to the sequence length distributions in both the hard and soft blocks and the overall fairly broad (M_w/M_n of at least 2) molecular weight distribution there are other molecular features which make segmented multiblock copolymers more complex than triblock copolymers. As suggested by Figure 3, the nanometer-scale microdomain geometry for random multiblock copolymers will involve a variety of domain sizes and shapes, as well as multiple loop and bridge conformations for the soft segments. Moreover, for many multiblock copolymers, the hard segment selected is crystalline, so that in addition to microphase separation, crystallization of the hard segment also serves to drive the self-assembly process. The soft segment can crystallize and/or hydrogen-bond with the hard segment, introducing yet another influence on the final morphology. Overall, primarily due to the lack of synthetic control, the complexity of the physical structure of random multiblock copolymers leads to rather less precise correlations for structure−property relationships than in the styrene−diene ABA TPEs. Many structural models used to describe the mechanical properties of segmented multiblocks are based on elasticity models of filled and unfilled rubbers[69] in contrast to anionically synthesized block copolymers, where small strain composite theory describes the mechanical response for several of the established morphologies quite well (see sections IV.2. and IV.4.).

IV. Styrenic Block Copolymers

Control of molecular and morphological characteristics in many early structure−property studies on block copolymers has been deficient. The Kraton family of polymers (Shell Oil Co.) have been the subject of numerous investigations, but only in some cases has it been acknowledged that the nominal triblock material contains with up to 20 wt % of diblock.[75] It is well-known that because of the absence of bridging midblock conformations, diblocks do not provide the mechanical strength that triblocks do[76] and thus significantly detract from the mechanical properties, especially at higher strains. Additionally, the influence of polydispersity in molecular weight is often neglected. Despite early claims to the contrary,[76−78] studies have shown an enhanced load-bearing capacity at large strains for larger molecular weight samples (at constant composition).[9,79] It may very well be that this molecular weight effect has been masked by the numerous other uncontrolled variables in early deformation studies. The microstructure of the rubber block has a significant impact on its glass transition temperature (e.g., T_g of 1,4-polybutadiene and 1,2-polybutadiene is −106 and −28 °C, respectively[80]) which will also affect mechanical properties. A detailed analysis of the rubber block microstructure, which strongly depends on the polymerization solvent and temperature, should also be reported.

Table 1. Block Copolymer Orientation Methods[a]

orientation method used	oriented materials used in deformation studies	oriented material used in other studies
extrusion	**13, 86, 121** 20, 21, 85, 122	123, 95, 124, 125
reciprocating shear	25, 91, 126	24, 29, 30, 32, 112, 127−132
press-molding	**37, 38,** 12	119
injection molding	**13, 96,** 11	
channel die		42, 60−62
couette		51, 52, 55, 56, 95
E-field		15, 16, 58, 59
rheometry		42−50, 133
roll-casting	92	39−41

[a] Bolded references indicate a study detailed in the text.

In addition to the synthetic structural variables, the morphological variables should also be controlled. These variables include those necessary for complete morphological characterization: domain type, domain and grain size, defect density, degree of orientation, etc. (recall Figure 1). Care should be taken in sample preparation. If an isotropic sample is desired, no bias which could lead to texturing should be allowed. Indeed, recent morphological studies have indicated that it is particularly difficult to prepare block copolymer samples with complete morphological isotropy due to substrate-induced orientation,[81] particularly at lower molecular weights where the morphology can be perturbed simply by handling.[82] If an anisotropic sample is desired, a preparation route must be used which induces a globally textured sample. Morphological probes of local regions would therefore be representative of the sample as a whole. In either the fully isotropic or the anisotropic case, a reproducible procedure of sample preparation should be used, as a large number of samples is generally necessary for accurate mechanical property measurements. This is especially true for anisotropic samples since a number of different loading geometries are of interest (e.g., see Figure 6).

Finally, in an ideal deformation study, one would monitor as a function of deformation those structural parameters which most influence the macroscopic response in the course of the mechanical deformation. A number of structure probes have been used in block copolymer deformation studies (see Table 2). These tools do indeed provide information on the morphology (transmission electron microscopy (TEM), small-angle X-ray scattering (SAXS), small-angle neutron scattering (SANS), light scattering, birefringence) and the molecule (infrared (IR) dichroism, birefringence, nuclear magnetic resonance (NMR), SANS) during measurement of mechanical properties (small strain: thermal expansion

Table 2. Structural Characterization Techniques Used in Deformation Studies[a]

technique	deformation study on oriented samples	deformation study on unoriented samples
SAXS	**37, 38, 86, 92,** 25, 41, 91, 126	**87, 98, 134**, 135, 136
SANS		**88**, 134
light scattering		87
birefringence	137, 124	85, 138−140
TEM	**86, 92**, 12, 20, 124	**13, 79, 97**, 83, 141, 142, 143, 144
IR dichroism		145
NMR		

[a] Bolded references indicate a study detailed in the text.

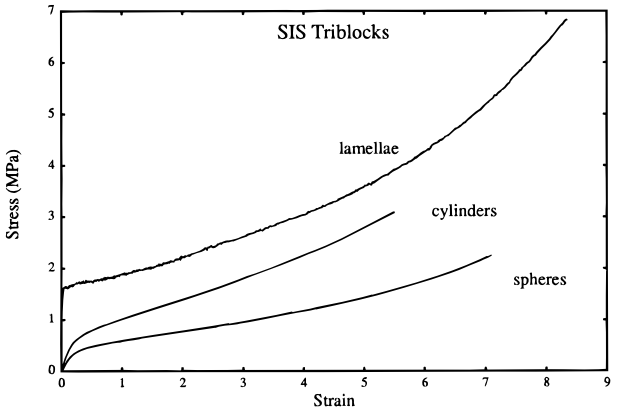

Figure 4. Stress−strain curves for polystyrene−polyisoprene−polystyrene (SIS) triblock copolymers cast without bias field. An increase in load-bearing capacity with increasing PS volume fraction is observed. Spheres: PS weight fraction 0.18, block molecular weights 10−89−10. Cylinders: PS weight fraction 0.30, block molecular weights 14−66−14. Lamellae: PS weight fraction 0.45, block molecular weights 22−29−22.

and modulus−temperature and modulus−frequency curves; large strain: stress−strain curves, yield point, ultimate stress/strain, stress relaxation, creep, toughness, swelling behavior, etc.). Unfortunately, it is fairly rare that several probes are combined in a particular deformation study. Many of the best studies which we highlight in this review do employ several characterization techniques. The most popular techniques include SAXS, birefringence, and TEM. The techniques can also be grouped according to whether they can be performed during the deformation process (SAXS, birefringence, light scattering) or whether some arresting procedure is necessary in order to freeze the morphology at a particular deformation before examination (TEM, NMR).

With the preparation of styrene−dienes of different morphologies came the (now obvious) realization that the microdomain geometry influences the mechanical response. The stress−strain curves for a series of unoriented Dexco SIS triblocks with varying amounts of the glassy PS phase are shown in Figure 4. The 18 wt % PS sample contains spherical regions of PS in a rubbery matrix, the 30 wt % PS sample exhibits a cylindrical PS microdomain geometry and the 45 wt % PS sample has a lamellar morphology. As can be seen from the data, the reinforcement by the PS of the rubbery matrix is dependent upon weight fraction PS. The initial modulus increases by factors of approximately 2 and 20 for the cylinder and lamellar morphologies over that for spheres. Of the three possible classical morphologies with rubber as a majority (or nearly majority) phase, the understanding of the influence of the glassy cylinder morphology on the mechanical response is most advanced. The cylinder morphology is the most prevalent morphology (in the range 20−30 wt % PS) in commercially available styrene−diene-based TPE materials, and not surprisingly more studies have been performed on cylinders than on either spheres or lamellae.

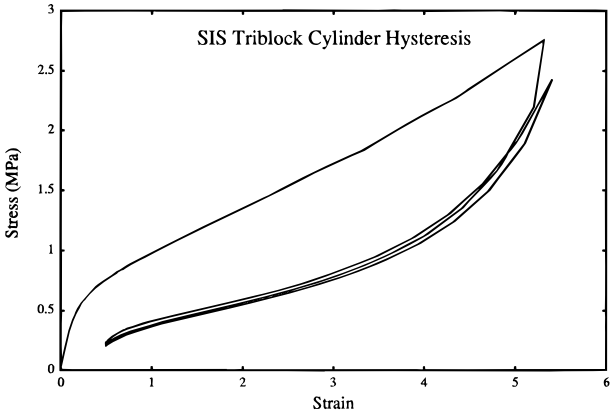

Figure 5. Two loading/unloading cycles of an SIS block copolymer with a cylindrical morphology (0.30 weight fraction PS). Note the drop in load-bearing capacity and lack of hysteresis in the second cycle. This deformation-induced change in mechanical property is known as "stress-softening".

There are a variety of deformation-related structural questions in styrene−diene systems that have been investigated with varying degrees of success. For example, one striking aspect observed in cyclic stress−strain traces of samples with glassy phase continuity in the stretching direction during the initial drawing is that of "stress softening". The initial deformation proceeds with high modulus and yielding and is often accompanied by necking. After relaxation, the second loading cycle exhibits a much more rubbery character with a significantly lower initial modulus and no yield point or necking phenomena (see Figure 5). Early studies speculated about a breakup of the PS "network" on the first draw.[83] The high modulus and yield point could be restored by annealing the sample at various temperatures before the second loading.[83−85] It was not, however, until highly oriented material became available that direct information of the cylinder breakup via TEM imaging provided a basis for the construction of detailed shear-lag models to compare with experimental stress−strain curves.[86]

Other deformation issues which have not nearly received enough attention to provide satisfactory explanations include some of the following: How do the respective A and B block chain dimensions respond to deformation in each of the microdomain morphologies? How does an increase in the molecular weight result in an increase in toughness at high strains? What is the interplay of molecular orientation and microdomain orientation at large strains? How does the morphology change at high strains? What is the bridging fraction (the ratio of effective midblock bridges to loops) in the various microdomain structures, how does this impact the mechanical properties, and how might this key molecular parameter be controlled? How well do composite models predict the moderate-to-large strain mechanical properties? Some of these questions have been examined, while some have not yet been broached. Next, we review some of the most significant deforma-

tion studies of each microdomain type, with a particular emphasis on oriented systems.

IV.1. Deformation Experiments on Spherical Morphologies. There have been only a few deformation studies of styrene−diene triblock copolymers with a morphology of PS spheres in a rubber matrix. The deformation process here is less affected by the microstructural features than with cylinders or lamellae, since the matrix phase is continuous across grain boundaries. There is no yield point or necking, as there is no continuous PS structure to break and the deformation is borne directly by the matrix chains at all strains. In this respect the molecular structure can be treated as a network of rubbery chains tied together by large multifunctional cross-link points. If the sample were to be macroscopically oriented, one would be in the unique position of knowing the relative locations of the cross-links.

Inoue et al.[87] were the first to perform a detailed study of the deformation process of a spherical morphology. A combination of light scattering, TEM and SAXS techniques were applied to a SIS triblock (23 wt % PS), a SI diblock (18.5 wt % PS), and the diblock blended with homo-PS and homo-PI. As expected, the triblock exhibited a much higher strength at high strains than either the diblocks or the diblock/homopolymer blends. The TEM micrographs of films cast from 5% toluene solutions clearly show discrete PS spheres which are (due to a lack of annealing) not on a ordered lattice. The SAXS data on the deformed diblock show an increase in spacing between spheres along the deformation direction and indicate that the deformation quickly becomes nonaffine. Light-scattering patterns (polarizer/analyzer parallel to the stretching direction) showed dramatic change with deformation. It is postulated that the origin of the scattering is due to density fluctuations at lower strains and void formation at higher strains. A model assuming spherical regions of high and low sphere density quantitatively describes the observed light scattering intensity patterns through part of the deformation. At the highest deformations, the low-density regions are thought to grow into microvoids which give rise to strong streaks in the scattering pattern along the stretching direction. The most prominent structural change in the deformation of the spherical morphology seems to be a long-range rearrangement of the spheres on length scales that give rise to the small-angle light scattering. Despite the lack of a long-range order in the samples, this study gives a very plausible explanation of the deformation process by combining a dynamic probe (light-scattering) with static probes (SAXS and TEM) of samples held at various stages of the deformation.

A small-angle neutron-scattering (SANS) study was recently carried out to determine the chain dimensions of the matrix blocks as a function of deformation in spherical triblocks.[88] A significant portion of the polyisoprene midblocks was randomly deuterated to eliminate scattering contrast between the PS domains and the PI matrix so that the molecular scattering of the matrix chains could be measured without the interparticle interference function (Bragg scattering of the PS spheres) dominating the pattern. Films were cast from dilute toluene solution but were not annealed. The radius of gyration (R_g) of the isoprene blocks was found to increase much more than would be expected for an affine deformation in the stretching direction, while the chain dimensions normal to the stretching direction hardly changed. It was conjectured that the movement of the PS domains is responsible for enhancing the local stress field, due to the local crowding of the rubbery bridging blocks as they orient themselves in the stretching direction. This would account for the larger-than-affine deformation of the matrix chains in the stretching direction. This is the first study (to our knowledge) to investigate the influence of deformation on the chain dimensions within a block copolymer in any morphology. Richards and Welsh reflect that preparation of macroscopically oriented samples would enable more information to be gained (for example, the molecular deformation as a function of crystallographic orientation).

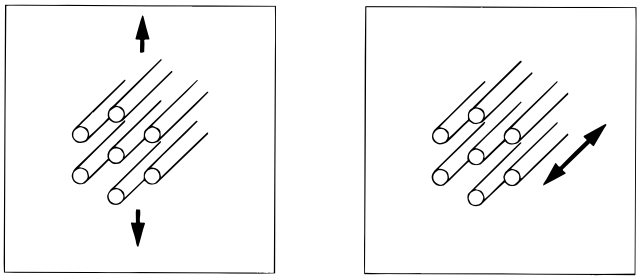

Figure 6. Two principal deformation directions in a cylindrical microdomain morphology, perpendicular to the cylinder axis and parallel to the cylinder axis.

Although a triblock copolymer with a spherical morphology has never been oriented on a macroscopic scale, poly(ethylenepropylene)−poly(ethylethylene) (PEP−PEE) diblocks containing PEE spheres have been successfully oriented.[29,89] It is found that large grains in a twin orientation[29] form during reciprocating shear orientation of an initially polygrain structure.

IV.2. Deformation Experiments on Cylindrical Morphologies. As mentioned previously, Keller and associates pioneered the area of structure−property relationships in oriented block copolymers. They modeled the small strain deformation behavior of a SBS sample with total molecular weight of 85 000 and 28 wt % PS as a composite of stiff fibers in a rubbery matrix. The elastic anisotropy of the oriented cylindrical morphology was completely characterized.[90] All five independent elastic constants were determined for this hexagonal crystal and the results compared to predictions of several fiber-reinforced composite theories.[90] The ratio of the moduli perpendicular and parallel to the cylinder axis was determined to be about 100.

A detailed study on the mechanical response of this system up to moderate (<120%) strains was performed by Odell and Keller using a combination of SAXS, TEM, and birefringence techniques.[86] Deformation in two principal directions was investigated (see Figure 6). It was found that the deformation in the direction perpendicular to the cylinders proceeded in an affine manner up to 20% strain, while that in the direction parallel to the cylinders (see Figure 6) was affine only up to about 3%, at which point the material yielded. [A later study[91] determined the limit of affine deformation in the perpendicular direction to be approximately 45% for a triblock of block molecular weights 7−35−7 (K).] A closer examination of the yielded material determined that the deformation in the necked region reached 80% before the neck propagated across the sample. The

necked region was found (from direct measurement of photographs of the necked region) to have a Poisson ratio of 0.48, essentially that of an incompressible rubber. Birefringence measurements on the necked region supported the argument that the butadiene carried most of the load after yield.

Finally and most significantly, direct evidence for the breakup of the PS cylinders was presented by Keller and Odell in TEM micrographs of a sample deformed by an unspecified amount in the direction parallel to the cylinders and then unloaded. Sample preparation involved deforming the material until a neck formed and subsequently storing the material in a strained condition until the stress had relaxed. Thereafter, the sample was hardened with OsO_4 and microtomed thin enough (~50 nm) so that "overlapping" cylinders in the 2-D projection did not complicate measurement of rod lengths. The TEM micrographs show a yielded section with the PS phase appearing as short rodlets approximately 70−110 nm in length but still macroscopically aligned. Although microscopic evidence of the structure of the deformed material had already been presented,[20] Odell and Keller's micrographs, together with their related experiments, presented a much clearer picture than did the earlier studies of the mechanical response of oriented cylinders to deformations up to about 80%. For deformation behavior beyond the yield point, composite theories were again applied to the system. Yielding was modeled as a progressive breaking of cylinders into shorter segments which can bear a higher load, borrowing a concept from composite theory known as shear lag. Another model with fewer assumptions, the "random break" model, gave values for the lengths of the broken rods that are in agreement with rod lengths measured in TEM images on material deformed to 80% strain.

IV.3. Large Strain Deformation of Oriented Cylinders. Samples with a globally oriented morphology provide an opportunity to observe the response of what is effectively a single grain to the imposed deformation. The first large-strain SAXS study of a press-molded block copolymer with a cylindrical morphology was conducted by Tarasov et al.[37] The SAXS patterns were recorded on photographic film and interpreted in terms of the breakup of the cylinders into long rodlets (which stay aligned) for parallel deformation and a breakup of the cylinders into a chevron-type structure for deformations perpendicular to the cylinder axis. The SAXS experiments hold particular interest, not only because they were the first large deformation studies but also because the incident beam was directed at several different angles with respect to the deformation direction giving different planar sections of the reciprocal space scattered intensity distribution. These patterns gave additional evidence for the interpretation that the texture of domains at large perpendicular deformation consisted of a zigzag chevron pattern (corresponding to a 4-point pattern in reciprocal space) of broken cylinders that were predominantly oriented at a particular angle with respect to the deformation direction (see Figure 8). This angle was determined to increase with deformation, reaching a value of 55° at a strain of 700%. Unfortunately the 3-D information carefully obtained by the authors in reciprocal space was not reconstructed self-consistently into a 3-D real space model.

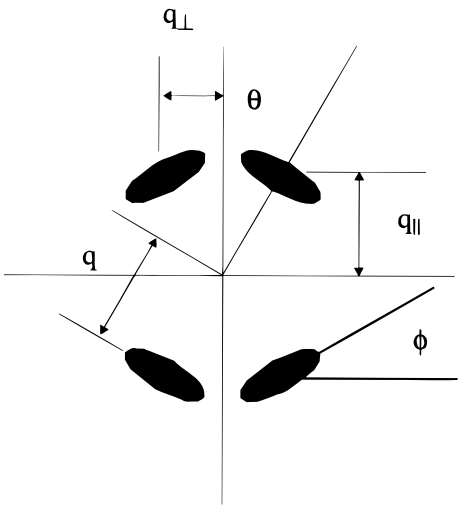

Figure 7. Schematic of a four-point pattern often observed in the SAXS of polymers. The radial distance q to the first lobe can be decomposed into a component parallel and perpendicular to the stretching direction (assumed vertical). The lobes themselves can be variously oriented.

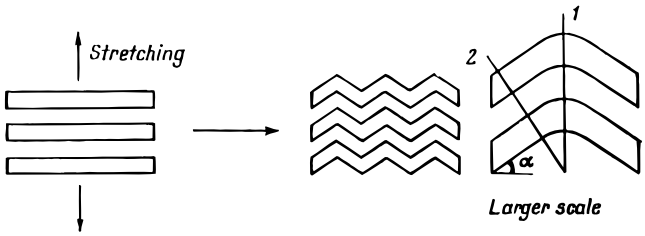

Figure 8. Schematic illustration of the changes of the hexagonal cylinder lattice in a monocrystal (longitudinal section is illustrated) when stretching is applied in a direction normal to the cylinder axis. Reprinted with permission.[37]

A more recent deformation study of oriented cylinders by SAXS considered the nature of the four-point pattern in more detail.[38] Four-point patterns, as often observed in the SAXS of polymers and liquid crystals, come in a great variety but generally consist of one or more intensity maxima in each of the four quadrants (see Figure 7). The main conclusion of Pakula et al.[38] based on X-ray investigations of samples oriented via press-molding, was that deforming oriented cylinders in *any* orientation with respect to the stretching direction results in the same final morphological state at high deformation: a chevron structure of broken cylinders. This "universal high deformation state" was also found for a sample which was initially comprised of a random orientation of grains. Again, at large (>100% strain) deformations, the same four-point pattern was observed. This indicated that the deformation behavior at large strains is controlled by the molecular orientation of the rubber blocks, while at low strains the deformation is controlled more by the initial morphological state. A serious limitation of this study was that the two-dimensional SAXS patterns were reconstructed using a one-dimensional detector scanned across the diffraction plane.

To better understand how the initial sample morphology influences the evolution of morphology at large strains,[92] we prepared near-single-crystal samples via roll-casting. SAXS and TEM confirm the high quality

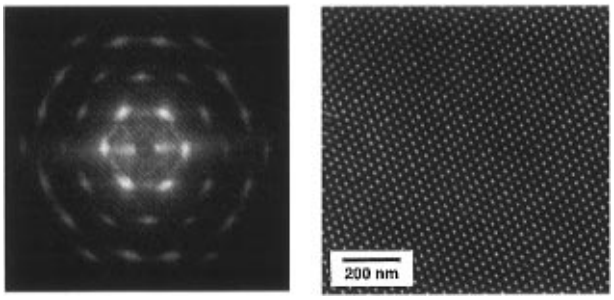

Figure 9. (a) SAXS pattern with the X-ray beam directed along the cylinder axis of a near-single-crystal sample of PS cylinders in a PI matrix. The SIS copolymer contains 30 wt % PS with block molecular weights of 14−66−14. The single-crystal nature of the sample is evident from the large number of well-resolved scattering peaks. (b) TEM image viewed in the cylinder axis direction of the same sample. The PS cylinders appear light and the PI matrix dark due to OsO_4 staining.

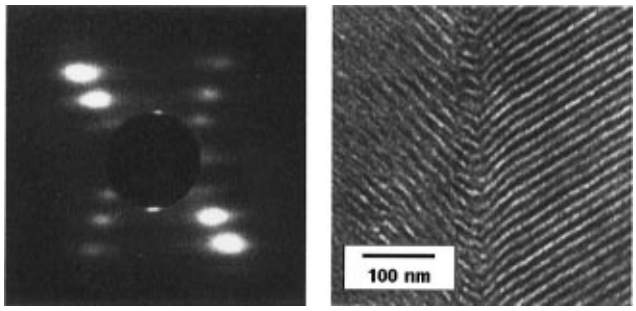

Figure 10. (a) SAXS pattern of an oriented triblock copolymer with a cylindrical morphology deformed in a direction transverse to the cylinder axis (vertical). The view direction is perpendicular to the cylinder axis. The pattern is taken from the same sample which yielded Figure 10b. (b) Bright-field electron micrograph of a cylindrical sample deformed perpendicularly to the cylinder axis to ∼400% strain, cross-linked with high-energy electrons and unloaded to 180% strain. The chevron texture observed here in the transverse view gives rise to the "X" pattern seen in Figure 10a. See text for further details.

of the initial sample orientation (see Figure 9). Two major challenges for investigating the morphology of the deformed state are the overall decrease in the sample scatter with increased deformation as exemplified by the disappearance of the high-q reflections, and the rapid stress relaxation at high strains and the recovery of the deformation upon unloading. To aid in the interpretation of the scattering pattern, a combined TEM-SAXS study permits the complementary information available from real and reciprocal space to be used in a self-consistent manner. To circumvent the viscoelastic effects of stress relaxation and creep recovery, an in situ dynamic technique such as synchrotron small-angle X-ray scattering can be used, but there is still the need to supplement the scattering data with TEM images. This means finding some way to arrest the deformed morphology so that TEM can be applied to samples deformed to various extents.

Synchrotron SAXS was performed on a single-crystal SIS (14−66−14) sample stretched along an axis normal to the direction of the cylinder axis. The transverse view shows that the meridional Bragg scattering changes into a cross (four-point pattern) as each reflection splits and moves off-axis toward lower q with increasing strain. This latter transformation occurs abruptly at strains of approximately 110%. On closer examination it is apparent that this "four-point pattern" contains several reflections (up to five) in each arm, indicating the preservation of a high degree of order at all stages of the deformation.

The sample in Figure 10b was prepared by cross-linking the isoprene phase using high-energy electrons while in the stretched state. Upon unloading from ∼400% strain, ∼180% strain remained. The TEM image shows a well defined tilt boundary (acute angle of approximately 70°) between regions of well-ordered parallel cylinders which were originally horizontal before the deformation. Figure 10a shows a 2-D SAXS pattern taken from the same cross-linked sample. The "X" pattern observed in deformation of cylindrical morphologies with the perpendicular deformation geometry can now be directly attributed to a cooperative bending of the glassy PS rods into a chevron-type structure. Additional SAXS and TEM taken at other angles reveals that a more complex structure exists than the simple 2-D chevron pattern. A full account of the 3-D morphology as a function of deformation and loading direction is in progress.[92]

These studies show that when a block copolymer consisting of a minority glassy component in a rubbery matrix component is deformed, there is a competition between chain orientation and domain orientation along the stretching direction. Thus in samples containing spherical or cylindrical PS microdomains, the strain is accommodated primarily in the soft rubbery matrix with the rubbery chains orienting along the stretch axis. In the case of glassy cylinders, the glassy domains tend to rotate their long axis toward the stretch axis. However, since the cylindrical domains in block copolymers have rather extraordinary L/D ratios (approximately 1000:1 for a polygrain structure and essentially infinite for the single-crystal samples), the reorientation process must be highly cooperative, involving whole grains or, as we have seen for the single-crystal samples, a breakup of the structure into a chevron morphology with a characteristic length scale on the order of microns. As is the case for polycrystalline deformation, compatibility[93] of the overall grain structure requires a complex deformational response, which varies from grain to grain.

IV.4. Deformation Experiments on Lamellar Morphologies. Using the same extrusion apparatus that they used for their work on oriented cylinders, Keller and co-workers were able to orient a lamellar-forming triblock into circular annuli of lamellae similar to the growth rings on a tree.[94] Later, however, a modification to the extrusion apparatus enabled sheet-oriented lamellae to be formed, which were subsequently used in a series of swelling studies.[95] However, no deformation studies were conducted.

An attempt to measure the five elastic constants of a highly oriented lamellar triblock was made by Allan et al.[96] An unusual injection molding process was used, as previous lamellar orientation methods did not yield samples of sufficient size and quality. A single-screw extruder was attached to a quadruple live-feed machine, which enabled the melt to be repeatedly sheared within the mold cavity. Although SAXS was not available to evaluate the global orientation, TEM micrographs showed highly oriented lamellae. As was done with the cylinder morphology, the modulus as a function of angle with

respect to the lamellar normal was compared against moduli obtained from composite theory using bulk values of the individual constituents, and an agreement reminiscent of the Arridge and Folkes[90] work on cylinders was demonstrated.

The large-strain deformation behavior of the lamellar morphology has not been studied as extensively as the cylindrical morphology. There has been only one study of the large strain behavior of *oriented* lamellae.[13] There have, however, been a number of studies of unoriented lamellae. With higher PS content, yielding and localized necking is expected to occur in lamellar samples, making precise determination of the local strain state difficult.

A commercial lamellar triblock sample for a deformation study using SAXS and TEM[97] was prepared by spin-casting followed by annealing at 60 °C. Although such a preparation technique yields a highly nonequilibrium structure, one notable result from the study is that TEM images of the deformed morphology were successfully obtained by staining the sample in a stretched state for 2 days. However, despite chemical stain-induced cross-linking, the samples contracted to 64% and 200%, from 85% and 500% strain, respectively. The micrographs show a chevron-like morphology at the smaller deformation and a chaotic morphology of broken polystyrene domains at the larger one. SAXS on the samples deformed beyond the yield point exhibits a characteristic four-point pattern attributed to fragmented lamellae, which are inclined to the stretching direction, in agreement with the chevron pattern visualized by TEM. At very large deformations, the SAXS patterns show "diffuse scattering", which Fujimura et al. interpreted as indicating that the broken PS domains are randomly dispersed in the PB matrix, with the PS reinforcing the rubber as a filler would in a composite.

Another deformation study of unoriented lamellae using SAXS showed the transformation of an initial isotropic ring of scattering in the undeformed region to a four-point lobe pattern within the necked region.[98] The interpretation of the mechanism of deformation is based on the observation that the relative amount of lateral contraction during uniaxial deformation indicates a constant volume process. It is suggested that necking proceeds through local extension and contraction of the rubber phase with little ductile deformation of the glassy phase. The position and orientation of the intensity lobes in the SAXS patterns as a function of draw ratio suggests a rotation of lamellar normals into the scattering direction. At large deformation the lobes of the four-point pattern continue to rotate at fixed azimuthal angle, leading Seguela and Prud'homme[98] to conclude that intragrain shearing of lamellae, in which the stacking axis orients into the stretching direction and lamellar normals remain in the preferred direction, is the most likely deformation mechanism at large deformation (see Figure 11).

A recent study by Yamaoka et al.[13] focused on the influence of compression molding and injection molding on mechanical properties. A K-resin (KR05 Phillips Petroleum) with an oriented lamellar morphology was deformed by tension, compression, and bending. TEM sections taken in three orthogonal directions of both the initial and deformed samples gave indication of the

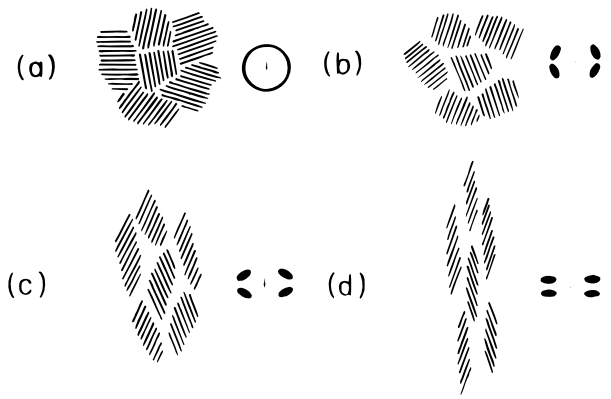

Figure 11. Schematic description of the grain arrangement at different stages of neck deformation together with the corresponding first-order diffraction maxima. Stretching direction vertical. Reprinted with permission from Seguela and Prud'homme.[98]

change in morphology with deformation. The initial oriented texture induced by the processing (and the subsequent cooling rate) influenced the stress−strain curve and the impact strength, as well as the flexural strength and modulus. This practical study clearly linked orientation to mechanical properties, but did not attempt to optimize the initial orientation or track the evolution of the morphology from the initial state as deformation proceeded. Unfortunately, the study suffers from the quality of the commercial material, which is reported to be "star-shaped", has a relatively large polydispersity and exhibits a nonequilibrium lamellar microdomain geometry at 25% PS.

V. Conclusions and Future Outlook

The elastic moduli and small strain response of ABA block copolymers organized into large near-single-crystal samples composed of glassy cylinders or of lamellae have been successfully measured and fit using composite theories. This approach adequately accounts for the role of the morphological response to the deformation in the small strain behavior of these thermoplastic elastomers.

Each of the three morphologies found in styrene−diene TPEs responds differently to deformation. The spherical morphology deformation process most parallels the deformation observed in an ideal network. Globally oriented samples with a cylindrical morphology behave anisotropically at both large and small strains. Though small-strain behavior is well understood, the well-ordered structure observed at large strain has not yet been fully explained. There have been too few large strain deformation studies on oriented lamellae for many conclusions to be drawn. Not only does the higher PS content result in localized deformation (necking), but it also reduces the time-dependent (viscoelastic) nature of the deformation.

Large-strain deformation carries both the morphology and the chain dimensions far from their equilibrium ground states. Molecular structural variables become more important once the glassy domain structure is broken. The exact nature of the relationship between domain structure and chain extension at large strains remains elusive. It is clear that a morphologically well-defined starting point will aid in the interpretation of the structure at large strains, as the dynamic evolution

of the morphology with deformation can be followed from this state to the unknown state using scattering experiments. Once the morphological structure at large deformations is made clear, the impact of synthetic variables, such as molecular weight,[9,99] effective bridging fraction,[100,101] chain architecture,[102,103] and chemical identity[104] on determining this structure and hence the large strain mechanical properties can be better evaluated.

Chain topology (midblock bridge vs loop conformations; diblock vs triblock) is expected to become important at large strains and at high temperatures[101,105−108] where the glassy domains no longer constrain the deformation. There has been little experimental work[88] and some theory[108−111] on the response of the rubbery chain to deformation for each type of morphology. Experimental measurement requires morphological control as well as chain labeling to increase signal in neutron-scattering experiments to follow the chain response. Spectroscopy methods (IR dichroism, NMR) give information on more local segmental motions, but these need to be combined with morphological measurements to enhance interpretation.

The determination of the macroscopic mechanical properties is only one area where the texturing or orientation of the morphology has aided in revealing molecular phenomena in TPEs. The measurement of the anisotropy of chain dimensions within the microdomain space of lamellar diblocks necessitates a highly oriented morphology.[112−119] The difference in the self-diffusion of diblocks parallel and perpendicular to the microdomain interface again requires macroscopically oriented samples.[120] Finally, as is common in determining the crystal structure of small and large molecules, effort is being made to prepare near-single-crystal material for the identification of new morphologies with scattering techniques.[30]

Future work will involve increased use of processing techniques in combination with an awareness of global equilibrium to produce well-characterized samples. Deformation studies, particularly in the large-strain region, will provide information toward answering some of the questions mentioned above. A basic understanding of structure−mechanical property relations of the relatively simple styrene−diene system will provide a context for deformation investigations of other TPEs. Increasing synthetic complexity can dramatically impact higher order morphological features (e.g., change the morphology diagram, influence chain conformation and domain structure). A procedure utilizing a combination of controlled chemistry, controlled morphology, and multiple characterization techniques will offer the best approach to unraveling the molecular and nanoscale influences on the small- and large-strain behavior of TPEs.

Acknowledgment. This work was supported by grants from NSF DMR 92-14853 and AFOSR F49620-94-1-0224. Prof. S. L. Gruner and Dr. D. A. Hajduk are acknowledged for providing the SAXS data for Figure 10b. C.C.H. thanks Benita Dair for critical review of the manuscript and Dr. Ramon Albalak for help with roll-casting. Work at BNL was supported by a grant from the DOE.

References

(1) Holden, G. In: *Thermoplastic Elastomers*; Legge, N. R., Holden, G., Schroeder, H. E., Eds.; Hanser: Munich, 1987; pp 481−506.
(2) Wolfe, J. R. J. In: *Thermoplastic Elastomers*; Legge, N. R., Holden, G., Schroeder, H. E., Eds.; Hanser Publishers: Munich, 1987; pp 117−131.
(3) Rader, C. P. In: *Modern Plastics: Encyclopedia 1996*; Kaplan, W. L., Ed.; McGraw-Hill Co.: New York, 1996; Vol. 72, pp B56−B58.
(4) Balsara, N. P.; Dai, H. J.; Watanabe, H.; Sato, T.; Osaki, K. *Macromolecules* **1996**, *29*, 3507−3510.
(5) Molau, G. E. In: *Block Polymers*; Aggarwal, S. L., Ed.; Plenum Press: New York, 1970; pp 79−106.
(6) Smith, T. L.; Dickie, R. A. *J. Polym. Sci. Part C* **1969**, *26*, 163−187.
(7) Robinson, R. A.; White, E. F. T. In: *Block Polymers*; Aggarwal, S. L., Ed.; Plenum Press: New York, 1970; pp 123−136.
(8) Akovali, G.; Diamant, J.; Shen, M. *J. Macromol. Sci.: Phys.* **1977**, *B13*, 117−131.
(9) Chen, Y.-D. M.; Cohen, R. E. *J. Appl. Polym. Sci.* **1977**, *21*, 629−643.
(10) Diamant, J.; Soong, D.; Williams, M. C. *Polym. Eng. Sci.* **1982**, *22*, 673−683.
(11) Ramsteiner, F.; Heckmann, W. *Polym. Commun.* **1984**, *25*, 178−179.
(12) Pedemonte, E.; Dondero, G.; de Candia, F.; Romano, G. *Polymer* **1976**, *17*, 72−76.
(13) Yamaoka, I.; Kimura, M. *Polymer* **1993**, *34*, 4399−4409.
(14) Seguela, R.; Prud'homme, J. *Macromolecules* **1988**, *21*, 635−643.
(15) Amundson, K.; Helfand, E.; Davis, D. D.; Quan, X.; Patel, S. S. *Macromolecules* **1991**, *24*, 6546−6548.
(16) Amundson, K.; Helfand, E.; Davis, D. D.; Quan, X.; Patel, S. S.; Smith, S. D. *Macromolecules* **1992**, *25*, 1200.
(17) Larson, R. G. *Rheol. Acta* **1992**, *31*, 497−520.
(18) Walker, B. *Handbook of Thermoplastic Elastomers*; Van Nostrand Reinhold: New York, 1979.
(19) Bhowmick, A. K.; Stephens, H. L. *Handbook of Elastomers: New Developments & Technology*; Marcel Dekker: New York, 1988.
(20) Pedemonte, E.; Turturro, A.; Dondero, G. *Brit. Polym. J.* **1974**, *6*, 277−282.
(21) LeBlanc, J. L. *J. Appl. Polym. Sci.* **1977**, *21*, 2419−2437.
(22) Riep, P. W. Ph.D. Thesis Brunel University, Uxbridge, Middle-Sex, England, 1983.
(23) Folkes, M. J.; Keller, A.; Scalisi, F. P. *Colloid Polym. Sci.* **1973**, *251*, 1−4.
(24) Skoulios, A. *J. Polym. Sci. Polym. Symp.* **1977**, *58*, 369−380.
(25) Manthis, A.; Hadziioannou, G.; Skoulios, A. *Polym. Eng. Sci.* **1977**, *17*, 570−572.
(26) Hadziioannou, G.; Mathis, A.; Skoulios, A. *Colloid Polym. Sci.* **1979**, *257*, 136−139.
(27) Hadziioannou, G.; Mathis, A.; Skoulios, A. *Colloid Polym. Sci.* **1979**, *257*, 15−22.
(28) Almdal, K.; Koppi, K. A.; Bates, F. S.; Mortenson, K. *Macromolecules* **1992**, *25*, 1743−1751.
(29) Koppi, K. A.; Tirrell, M.; Bates, F. S. *J. Rheol.* **1994**, *38*, 999−1027.
(30) Mortensen, K.; Almdal, K.; Bates, F. S.; Koppi, K.; Tirrell, M.; Norden, B. *Physica B* **1995**, *213* and *214*, 682−684.
(31) Muller, R.; Pesce, J. J.; Picot, C. *Macromolecules* **1993**, *26*, 4356−4362.
(32) Okamoto, S.; Saijo, K.; Hashimoto, T. *Macromolecules* **1994**, *27*, 5547−5555.
(33) Cates, M. E.; Milner, S. T. *Phys. Rev. Lett.* **1989**, *62*, 1856−1859.
(34) Fredrickson, G. H. *J. Rheol.* **1994**, *38*, 1045−1067.
(35) Koppi, K. A.; Tirrell, M.; Bates, F. S. *Phys. Rev. Lett.* **1993**, *70*, 1449−1452.
(36) Pedemonte, E.; Dondero, G.; Alfonso, G.; de Candia, F. *Polymer* **1975**, *16*, 531−538.
(37) Tarasov, S. G.; Tsvankin, D. Y.; Godovsky, Y. K. *Polym. Sci. USSR* **1978**, *20*, 1728−1739.
(38) Pakula, T.; Saijo, K.; Kawai, H.; Hashimoto, T. *Macromolecules* **1985**, *18*, 1294−1302.
(39) Albalak, R. J.; Thomas, E. L. *J. Polym. Sci. Part B: Polym. Phys.* **1993**, *31*, 37−46.
(40) Albalak, R. J.; Thomas, E. L. *J. Polym. Sci. Part B: Polym. Phys.* **1994**, *32*, 341−350.
(41) Albalak, R. J. *Polymer* **1994**, *35*, 4115−4119.
(42) Scott, D. B.; Waddon, A. J.; Lin, Y.-G.; Karasz, F. E.; Winter, H. H. *Macromolecules* **1992**, *25*, 4175−4181.
(43) Morrison, F.; Bourvellec, G. L.; Winter, H. H. *J. Appl. Polym. Sci.* **1987**, *33*, 1585−1600.
(44) Morrison, F. A.; Winter, H. H. *Macromolecules* **1989**, *22*, 3533−3539.
(45) Morrison, F. A.; Winter, H. H.; Gronski, W.; Barnes, J. D. *Macromolecules* **1990**, *23*, 4200−4205.
(46) Winey, K. I.; Patel, S. S.; Larson, R. G.; Watanabe, H. *Macromolecules* **1993**, *26*, 2542−2549.

(47) Winey, K. I.; Patel, S. S.; Larson, R. G.; Watanabe, H. *Macromolecules* **1993**, *26*, 4373−4375.
(48) Larson, R. G.; Winey, K. I.; Patel, S. S.; Watanabe, H.; Bruinsma, R. *Rheol. Acta* **1993**, *32*, 245−253.
(49) Zhang, Y.; Wiesner, U.; Spiess, H. W. *Macromolecules* **1995**, *28*, 778.
(50) Zhang, Y.; Wiesner, U. *J. Chem. Phys.* **1995**, *103*, 4784.
(51) Terrisse Ph.D. Thesis; Universite Louis Pasteur de Strasbourg, 1973.
(52) Morrison, F. A.; Mays, J. W.; Muthukumar, M.; Nakatani, A. I.; Han, C. C. *Macromolecules* **1993**, *26*, 5271−5273.
(53) Jackson, C. L.; Barnes, K. A.; Morrison, F. A.; Mays, J. W.; Nakatani, A. I.; Han, C. C. *Macromolecules* **1995**, *28*, 713−722.
(54) Jackson, C. L.; Morrison, F. A.; Nakatani, A. I.; Mays, J. W.; Muthukumar, M.; Barnes, K. A.; Han, C. C. In: *Flow-Induced Structure in Polymers*; Nakatani, A. I., Dadmun, M. D., Eds.; ACS: Washington, DC, 1995; Vol. 597, pp 233−245.
(55) Balsara, N. P.; Hammouda, B.; Kesani, P. K.; Jonnalagadda, S. V.; Straty, G. C. *Macromolecules* **1994**, *27*, 2566−2573.
(56) Balsara, N. P.; Hammouda, B. *Phys. Rev. Lett.* **1994**, *72*, 360−363.
(57) Le Meur, J.; Terrisse, J.; C., S. e. G. *J. Phys. Colloque C5* **1971**, *32*, 301−304.
(58) Amundson, K.; Helfand, E.; Quan, X.; Smith, S. D. *Macromolecules* **1993**, *26*, 2698−2703.
(59) Amundson, K.; Helfand, E.; Quan, X.; Hudson, S. D.; Smith, S. D. *Macromolecules* **1994**, *27*, 6559−6570.
(60) Kofinas, P.; Cohen, R. E. *Macromolecules* **1994**, *27*, 3002−3008.
(61) Cohen, R. E.; Bellare, A.; Drzewinski, M. A. *Macromolecules* **1994**, *27*, 2321−2323.
(62) Kofinas, P.; Cohen, R. E. *Macromolecules* **1995**, *28*, 336−343.
(63) Galeski, A.; Argon, A. S.; Cohen, R. E. *Macromolecules* **1991**, *24*, 3953−3961.
(64) Galeski, A.; Bartczak, Z.; Argon, A. S.; Cohen, R. E. *Macromolecules* **1992**, *25*, 5705−5718.
(65) Song, H. H.; Argon, A. S.; Cohen, R. E. *Macromolecules* **1990**, *23*, 870−876.
(66) Bellare, A.; Cohen, R. E.; Argon, A. S. *Polymer* **1993**, *34*, 1393−1403.
(67) Tonelli, C.; Trombetta, T.; Scicchitano, M.; Simeone, G.; Ajroldi, G. *J. Appl. Polym. Sci.* **1996**, *59*, 311−327.
(68) Fodor, Z.; Faust, R. *J. Macromol. Sci. Pure Appl. Chem.* **1996**, *A33*, 305−324.
(69) Petrovic, Z. S.; Ferguson, J. *Prog. Polym. Sci.* **1991**, *16*, 695−836.
(70) Meckel, W.; Goyert, W.; Wieder, W. In: *Thermoplastic Elastomers: A Comprehensive Review*; Legge, N. R., Holden, G., Schroeder, H. E., Eds.; Hanser: Munich, 1987; pp 13−46.
(71) Odian, G. *Principles of Polymerization*; John Wiley & Sons: New York, 1991.
(72) Flory, P. J. *Principles of Polymer Chemistry*; Cornell University Press: Ithaca, NY, 1953.
(73) Eisenbach, C. D.; Heinemann, T.; Ribbe, A.; Stadler, E. *Angew. Makromol. Chem.* **1992**, *202/203*, 221−241.
(74) Eisenbach, C. D.; Stadler, E. *Macromol. Chem. Phys.* **1995**, *196*, 1981−1997.
(75) Fetters, L. J.; Meyer, B. H.; McIntyre, D. *J. Appl. Polym. Sci.* **1972**, *16*, 2079−2089.
(76) Morton, M. In: *Encyclopedia of Polymer Science and Technology*; Bikales, M., Ed.; Wiley-Interscience: New York, 1971; Vol. 15, pp 508−530.
(77) Holden, G.; Bishop, E. T.; Legge, N. R. *J. Polym. Sci. Part C* **1969**, *26*, 37−57.
(78) Holden, G. In: *Encyclopedia of Polymer Science and Engineering*; Mark, H. F., Bikales, M., Overberger, C. G., Menges, G., Kroshwitz, J. I., Eds.; John Wiley & Sons: New York, 1986; Vol. 5, pp 416−430.
(79) Hashimoto, T.; Fujimura, M.; Saijo, K.; Kawai, H.; Diamant, J.; Shen, M. In: *Multiphase Polymers*; Cooper, S. L., Estes, G. M., Eds.; ACS Advances in Chemistry Series: 1979; pp 257−275.
(80) Tate, D. B.; Bethea, T. W. In: *Encyclopedia of Polymer Sciene and Technology*; Mark, H. F., Bikales, M., Overberger, C. G., Menges, G., Eds.; John Wiley & Sons: New York, 1986; Vol. 2, pp 538−590.
(81) Hasegawa, H.; Tanaka, H.; Hashimoto, T.; Han, C. C. *Macromolecules* **1987**, *20*, 2120.
(82) Hajduk, D. A.; Harper, P. E.; Gruner, S. M.; Honeker, C. C.; Thomas, E. L.; Fetters, L. J. *Macromolecules* **1995**, *28*, 2570−2573.
(83) Beecher, J. F.; Marker, L.; Bradford, R. D.; Aggarwal, S. L. *J. Polym. Sci. Part C* **1969**, *26*, 117−134.
(84) Kelterborn, J. C.; Soong, D. S. *Polym. Eng. Sci.* **1982**, *22*, 654−672.
(85) Canevarolo, S. V.; Birley, A. W.; Hemsley, D. A. *Brit. Polym. J.* **1986**, *18*, 60−64.
(86) Odell, J. A.; Keller, A. *Polym. Eng. Sci.* **1977**, *17*, 544−559.
(87) Inoue, T.; Moritani, M.; Hashimoto, T.; Kawai, H. *Macromolecules* **1971**, *4*, 500−507.
(88) Richards, R. W.; Welsh, G. *Eur. Polym. J.* **1995**, *31*, 1197−1206.
(89) Almdal, K.; Koppi, K. A.; Bates, F. S. *Macromolecules* **1993**, *26*, 4058−4060.
(90) Arridge, R. G. C.; Folkes, M. J. *J. Phys. Part D: Appl. Phys.* **1972**, *5*, 344−358.
(91) Hadziioannou, G.; Mathis, A.; Skoulios, A. *Colloid Polym. Sci.* **1979**, *257*, 337−343.
(92) Honeker, C. C.; Thomas, E. L. Manuscript in preparation.
(93) Malvern, L. E. *Introduction to the Mechanics of a Continuous Medium*; Prentice-Hall: Englewood Cliffs, NJ, 1969.
(94) Dlugosz, J.; Folkes, M. J.; Keller, A. *J. Polym. Sci. Part B: Polym. Phys.* **1973**, *11*, 929−938.
(95) Folkes, M. J.; Keller, A. *J. Polym. Sci. Part B: Polym. Phys.* **1976**, *14*, 833−846.
(96) Allan, P.; Arridge, R. G. C.; Ehtaiatkar, F.; Folkes, M. J. *J. Phys. D* **1991**, *24*, 1381−1390.
(97) Fujimura, M.; Hashimoto, T.; Kawai, H. *Rubber Chem. Technol.* **1978**, *51*, 215−224.
(98) Seguela, R.; Prud'homme, J. *Macromolecules* **1981**, *14*, 197−202.
(99) Bard, J. K.; Chung, C. I. In: *Thermoplastic Elastomers: A Comprehensive Review*; Legge, N. R., Holden, G., Schroeder, H. E., Eds.; Hanser: Munich, 1987; pp 303−323.
(100) Brinkmann, S.; Stadler, R. Personal communication, 1996.
(101) Watanabe, H. *Macromolecules* **1995**, *28*, 5006−5011.
(102) Bi, L.-K.; Fetters, L. J. *Macromolecules* **1976**, *9*, 732−742.
(103) Bi, L.-K.; Fetters, L. J.; Morton, M. *Polym. Prepr. ACS Polym. Chem. Div.* **1974**, *15*, 157−163.
(104) Li, D.; Faust, R. *Macromolecules* **1995**, *28*, 4893−4898.
(105) Zhulina, E. B.; Halperin, A. *Macromolecules* **1992**, *25*, 5730−5741.
(106) Matsen, M. W.; Schick, M. *Macromolecules* **1994**, *27*, 187−192.
(107) Matsen, M. W. *J. Chem. Phys.* **1995**, *102*, 3884−3887.
(108) Turner, M. S. *Macromolecules* **1995**, *28*, 6878−6882.
(109) Wang, Z.-G. *J. Chem. Phys.* **1994**, *100*, 2298−2309.
(110) Hamley, I. W. *Phys. Rev. E* **1994**, *50*, 2872−2880.
(111) Amundson, K.; Helfand, E. *Macromolecules* **1993**, *26*, 1324−1332.
(112) Hadziioannou, G.; Picot, C.; Skoulios, A.; Ionescu, M.-L.; Mathis, A.; Duplessix, R.; Gallot, Y.; Lingelser, J.-P. *Macromolecules* **1982**, *15*, 263−267.
(113) Hasegawa, H.; Hasimoto, T.; Kawai, H.; Lodge, T. P.; Amis, E. J.; Glinka, C. J.; Han, C. C. *Macromolecules* **1985**, *18*, 67−78.
(114) Hasegawa, H.; Tanaka, H.; Hashimoto, T.; Han, C. C. *Macromolecules* **1987**, *20*, 2120−2127.
(115) Matsushita, Y.; Nakao, Y.; Saguchi, R.; Mori, K.; Choshi, H.; Muroga, Y.; Noda, I.; Nagasawa, M.; Chang, T.; Glinka, C. J.; Han, C. C. *Macromolecules* **1988**, *21*, 1802−1806.
(116) Matsushita, Y.; Mori, K.; Saguchi, R.; Noda, I.; Nagasawa, M.; Chang, T.; Glinka, C. J.; Han, C. C. *Macromolecules* **1990**, *23*, 4387−4391.
(117) Matsushita, Y.; Mori, K.; Mogi, Y.; Saguchi, R.; Moda, I.; Hagasawa, M. *Macromolecules* **1990**, *23*, 4317−4321.
(118) Matsushita, Y.; Nomura, M.; Noda, I.; Imai, M. *Physica B* **1995**, *213* and *214*, 697−699.
(119) Koizumi, S.; Hashimoto, T. *Physica B* **1995**, *213* and *214*, 703−706.
(120) Dalvi, M. C.; Lodge, T. P. *Macromolecules* **1993**, *26*, 859−861.
(121) Keller, A.; Odell, J. A. In: *Processing, Structure and Properties of Block Copolymers*; Folkes, M. J., Ed.; Elsevier Applied Science: New York, 1985.
(122) Kraus, G.; Rollmann, K. W. *J. Macromol. Sci. Phys.* **1980**, *B17*, 407−425.
(123) Keller, A.; Pedemonte, E.; Willmouth, F. M. *Nature* **1970**, *225*, 538−539.
(124) Folkes, M. J.; Keller, A.; Odell, J. A. *J. Polym. Sci. Part B: Polym. Phys.* **1976**, *14*, 847−859.
(125) Arridge, R. G. C.; Folkes, M. J. In: *Processing, Structure and Properties of Block Copolymers*; Folkes, M. J., Ed.; Elsevier Applied Science: New York, 1985; pp 125−164.
(126) Hadziioannou, G.; Mathis, A.; Skoulios, A. *Colloid Polym. Sci.* **1979**, *257*, 344−350.
(127) Koppi, K. A.; Tirrell, M.; Bates, F. S.; Almdal, K.; Colby, R. H. *J. Phys. II (France)* **1992**, *2*, 1941−1959.
(128) Förster, S.; Khandpur, A. K.; Zhao, J.; Bates, F. S.; Hamley, I. W.; Ryan, A. J.; Bras, W. *Macromolecules* **1994**, *27*, 6922−6935.
(129) Hamley, I. W.; Koppi, K. A.; Rosedale, J. H.; Bates, F. S.; Almdal, K.; Mortenson, K. *Macromolecules* **1993**, *26*, 5959−5970.
(130) Hamley, I. W.; Gehlsen, M. D.; Khandpur, A. K.; Koppi, K. A.; Rosedale, J.; Schulz, M. F.; Bates, F. S.; Almdal, K.; Mortensen, K. *J. Phys. II (France)* **1994**, *4*, 2161−2186.
(131) Schulz, M. F.; Bates, F. S.; Almdal, K.; Mortensen, K. *Phys. Rev. Lett.* **1994**, *73*, 86−89.
(132) Lehrke, J.; Crämer, K.; Küchow, H.; Gronski, W. *Makromol. Chem.: Rapid Commun.* **1990**, *11*, 495−499.
(133) Winey, K. I.; Gobran, D. A.; Xu, Z.; Fetters, L. J.; Thomas, E. L. *Macromolecules* **1994**, *27*, 2392−2397.
(134) Richards, R. W.; Mullin, J. T. In: *Scattering, Deformation, and Fracture in Polymers*; Wignall, G. D., Crist, B., Russell, T. P., Thomas, E. L., Eds.; Materials Research Society: Pittsburgh, 1987; Vol. 79, pp 299−308.

(135) Polizzi, S.; Stribeck, N.; Zachmann, H. G.; R., B. *Colloid Polym. Sci.* **1989**, *267*, 281−291.
(136) Polizzi, S.; Boesecke, P.; Stribeck, N.; Zachmann, H. G.; Bordeiau, R. *Polymer* **1990**, *31*, 638−645.
(137) Folkes, M. J.; Keller, A. *Polymer* **1971**, *12*, 222−236.
(138) Henderson, J. F.; Grundy, K. H.; Fischer, E. *J. Polym. Sci. Part C* **1968**, *16*, 3121−3131.
(139) Fischer, E.; Henderson, J. F. *J. Polym. Sci. Part C* **1969**, *26*, 149−160.
(140) Wilkes, G. L.; Stein, R. S. *J. Polym. Sci. Part A-2* **1969**, *7*, 1525−1537.
(141) Hendus, H.; Illers, K.-H.; Ropte, E. *Colloid Polym. Sci.* **1966**, *216*−217, 110−119.
(142) Kotaka, T.; Tetsuhiro, M.; Arai, K. *J. Macromol. Sci. Phys.* **1980**, *B17*, 303−336.
(143) Zhao, Y. *Macromolecules* **1992**, *25*, 4705−4711.
(144) Sakamoto, J.; Sakurai, S.; Doi, K.; Nomura, S. *Polymer* **1993**, *34*, 4837−4840.
(145) Gronski, W.; Emeis, D.; Brüderlin, A.; Jacobi, M. M.; Stadler, R.; Eisenbach, C. D. *Brit. Polym. J.* **1985**, *17*, 103−110.

CM960146Q